Sound & Vibration 2026, 60(5), 4339.
doi: https://doi.org/10.59400/sv4339

Article

Dynamics of high-rise axisymmetric structures

Mirziyod Mirsaidov[1], Sherzod Khudainazarov[1], Muhsin Teshaev[2,*], Talibjan Sabirjanov[3], Bakhtiyor Urinov[1], Ozodakhon Khaydarova[3]

[1] Mechanics and Computer Modeling Department, "Tashkent Institute of Irrigation and Agricultural Mechanization Engineers" National Research University, Tashkent 100000, Uzbekistan

[2] Bukhara Branch of Institute of Mathematics named after V.I. Romanivskii, Uzbekistan Academy of Sciences, Bukhara 200100, Uzbekistan

[3] Applied Mechanics Department, Fergana Polytechnic Institute, Fergana 150100, Uzbekistan

* **Corresponding author:** Muhsin Teshaev, muhsin_5@mail.ru

CITATION

Mirsaidov M, Khudainazarov S, Teshaev M, et al. Dinamics of high-rise axisymmetric structures. Sound & Vibration. 2026; 60(5): 4339. https://doi.org/10.59400/sv4339

ARTICLE INFO

Received: 28 April 2026
Revised: 26 June 2026
Accepted: 13 July 2026
Available online: 14 August 2026

Abstract: The article discusses the natural and forced oscillations of a "high-rise structure - dynamic vibration damper" system, focusing on its dynamic interactions. A mathematical model of this system has been developed, along with a calculation methodology, a numerical implementation algorithm, and a corresponding computer program that utilizes complex arithmetic tools for an accurate description of dynamic processes. Special attention was given to the viscoelastic properties of the structural material. The Boltzmann-Volterra hereditary law was applied to more accurately describe the time-dependent deformation characteristics. A practical example was explored using the high-rise smokestack of the Novo-Angren thermal power plant, which stands at 330 m tall. The natural oscillation frequencies of this structure were determined, and amplitude-frequency characteristics were constructed accounting for the presence of dynamic dampers and various kinematic impacts. During the problem-solving process, an analysis was conducted on how the parameters of both the structure and the effectiveness of the dynamic vibration damper (DVD) influence the system's response. Various combinations of system parameters were examined to identify patterns in changes to the dynamic response. Based on this research, optimal parameters for dynamic damping of oscillations were established for the real structure, leading to effective reductions in oscillation amplitudes and an increase in the reliability of the structure's operation under dynamic influences. Keywords: high-rise axi

Keywords: high-rise axisymmetric structures; dynamic vibration damper; viscoelasticity; natural frequency; amplitude-frequency response (AFR)

1. Introduction

The importance of designing and constructing high-rise buildings is driven by several key factors. These include the optimization of land use and the reduction of operational costs through efficient structural designs and aerodynamics. High-rise buildings serve as architectural landmarks and symbols for cities, attracting tourists and enhancing their appeal. Additionally, they must prioritize safety, environmental sustainability, durability, and economic efficiency. Innovative technologies, new materials, and intelligent control systems are increasingly applied to enhance the design and construction processes of these structures.

High-rise buildings are essential components of modern infrastructure, necessitating innovative approaches to ensure their safety, efficiency, and sustainability.

Evaluating the dynamic behavior of these structures when subjected to seismic and dynamic loads is crucial for guaranteeing their strength and long-term durability. Such loads can impose significant stresses and strains, potentially leading to structural failure.

Dynamic vibration dampers (DVDs) are commonly used to reduce vibration amplitudes in high-rise buildings. While various design solutions and calculation methods for DVDs have been developed, the assessment of their effectiveness in certain building designs still requires further investigation. When utilizing a DVD to mitigate vibrations, challenges can arise in the calculation methods, particularly concerning the actual geometry of the structure, the material's deformation properties, and other parameters related to both the building and the dynamic damper. It is essential to regulate the dissipative properties of the entire system and to optimize the DVD parameters to achieve the maximum possible damping effectiveness.

Allena and Bhavani Chowdary [1] studied the natural vibrations of high-rise structures, taking into account the effects of mass and geometric irregularities on their seismic response. The objects of the study are high-rise buildings with regular (R) and geometrically irregular stepped (GIR) shapes, up to 18 stories high, made of reinforced concrete. The novelty of this research lies in identifying patterns of damage localization and examining how the position of irregularities affects the dynamic stability of buildings.

In the study by Ivankova et al. [2], wall and frame systems were compared, and the effects of dilatation and joints in individual building components were analyzed. The results indicated that alterations in the load-bearing system significantly influence the horizontal displacements and natural frequencies of structures, particularly under seismic loads.

Aihemaiti et al. [3] examined changes in the natural frequencies, attenuation coefficients, and curvature of the first four longitudinal vibration modes of a 50-story skyscraper in Kunming, China. This analysis is based on continuous monitoring data collected over 39 months, which included a period during which 35 earthquakes occurred. The study found that the building's natural frequencies correlated significantly with temperature, absolute humidity, and wind speed, while the impact of precipitation was nearly negligible.

One of the key areas of dynamics is the nonlinear dynamics of thin shells. Foroutan and Dai [4] investigated the nonlinear dynamics of functionally graded thin shells reinforced with inclined stiffeners and subjected to external excitation. The properties of the material vary across the thickness in accordance with the power-law distribution of volume fractions. The use of the Galerkin method reduces the original problem to a nonlinear dynamic system with two degrees of freedom, containing quadratic and cubic nonlinearities, and accounting for external excitation.

Xue and Hao [5] examined the transverse vibrations of high-rise buildings subjected to vortex shear conditions, where nonlinear aerodynamic damping plays a significant role. To assess aerodynamic damping, an analytical approach was proposed that analyzes the probabilistic characteristics of the amplitude of stochastic vibrations across various structural damping values. The study investigates the impact of the response range and uncertainties on the displacement probability density function.

The effect of fluid viscous dampers on the dynamic behavior of a 30-story reinforced concrete high-rise building is studied by Patil and Salgar [6]. The building model was developed using the ETABS 2018 software package, and the seismic analysis was performed using the response spectrum method in accordance with the requirements of IS 1893–2016 standards. Using the Python programming language, the optimal damper placement was determined, and the dynamic performance of the reinforced concrete high-rise building was compared with that of the building without dampers.

A significant scientific approach to reducing vibrations caused by seismic and periodic effects is the use of tuned mass dampers (TMDs). The effectiveness of TMDs in mitigating wind and seismic vibrations in high-rise structures was examined by Tudu et al. [7]. The ETABS software package was utilized to analyze two structures, each 120 m tall—a pyramidal structure and a square structure—designed according to Indian standards. High efficiency of TMDs and their potential application in the design of high-rise buildings in regions prone to strong winds and cyclones were confirmed.

A vibration protection scheme that includes a dynamic vibration damper installed on one of the floors of the protected structure was developed by Mondrus et al. [8]. The calculation model is represented as an elastic rod with concentrated masses at various floor levels, taking into account both force and kinematic effects.

Legeza and Neshchadym [9–11] investigated the forced vibrations of these buildings. To analyze their dynamic response, the authors developed mathematical models represented by systems of nonlinear differential equations. The findings indicate that with optimally configured parameters for the pendulum dampers, the amplitude of forced vibrations can be reduced by more than five times.

The development of pendulum damper designs is the subject of the study by Aly and Chapain [12], where the dynamics of a 5 MW wind turbine, subjected to seismic impacts, is investigated. The study focused on a system with a new pendulum impact damper designed to reduce structural vibrations. The MATLAB software package was used to determine the optimal damper parameters.

Akyürek [13] and Kontoni and Farghaly [14] investigated ways to improve the dynamic stability of high-rise buildings with various geometric shapes under wind and seismic forces using dynamic vibration dampers. The research focused on high-rise structures made from steel and reinforced concrete, each with different structural designs. The authors analyzed how factors such as building shape, material properties, wind direction, and spatial asymmetry influence the effectiveness of the dynamic dampers.

Friction dampers, which serve as connecting elements between the frame and wall structures, have been proposed by Quintana Gallo et al. [15]. Their effectiveness was evaluated using nonlinear numerical modeling, comparing the dynamic behavior of hybrid wood-steel structures both with and without friction dampers.

Ding et al. [16] discussed both theoretical and experimental investigations of annular, toroidal, adjustable fluid viscous dampers. These dampers were examined in engineering structures subjected to seismic impacts, and the effectiveness of multi-mode vibration-damping systems was evaluated. The studies established that fluid viscous dampers significantly reduce horizontal vibrations in structures.

The 183-m-tall smokestack at the Rugeley Power Station was examined by Brownjohn et al. [17–19]. A dynamic vibration damper was installed to enhance the damping properties of the structure and ensure its safe operation. The results indicated the high effectiveness of the dynamic damper in minimizing the dynamic response of the structure, thus ensuring its operational reliability.

The dynamics of a 295-m-tall industrial reinforced concrete smokestack at the Belchatow Power Plant (Poland) was examined by Górski [20]. The object under study was a thin-walled conical structure with a variable wall thickness along its height. To assess the dynamic behavior of the structure, field tests were conducted using accelerometers and GPS measurements of the horizontal displacements of the smokestack's upper section under wind loads.

Xiong and Niu [21] focused on the experimental determination of the dynamic characteristics of a unique high-rise structure, specifically examining the horizontal vibrations of the 597-m-tall Tianjin Tower. The study utilized RTK-GNSS technology to record the dynamic parameters, combined with digital signal processing methods such as the Chebyshev filter of the first kind and the Savitzky–Golay method.

The study outlined by Elias et al. [22] examined the behavior of smokestacks approximately 250 m in height, which were equipped with dynamic vibration dampers and subjected to seismic loading. The structural models were represented by systems of beam elements with multiple degrees of freedom.

The study of oscillatory processes in plate elements with attached masses under various dynamic loads constitutes a distinct field within the dynamics of mechanical systems. Safarov et al. [23] demonstrated that the developed mathematical model, based on the Boltzmann-Volterra hereditary theory of viscoelasticity, captures the oscillations in viscoelastic plates with attached masses. It has been established that concentrated masses reduce natural frequencies by up to 20%, while the use of viscoelastic damping elements reduces impulse loads by up to 25% and resonant oscillation amplitudes by 40–50%. These findings can be applied to the design of vibration-resistant plate structures and radio-electronic equipment operating under dynamic conditions.

One of the modern areas of scientific research is the development of new designs for dynamic vibration dampers. The low-frequency dynamic characteristics of new viscoelastic dampers were investigated by Alhasan et al. [24] and Liao et al. [25]. To evaluate the properties of various viscoelastic materials, experimental tests and numerical studies were conducted using modern ABAQUS and ANSYS software packages.

Wang et al. [26] examined the optimal design of adjustable dynamic vibration dampers for high-rise structures operating under seismic loads. Particular attention was paid to determining the optimal parameters of multi-adjustable mass vibration dampers. The results showed that the use of such systems could significantly reduce the amplitude of forced vibrations and improve the effectiveness of vibration protection for high-rise structures.

Arabzai et al. [27] presented a comprehensive review of modern damping systems for mitigating wind- and earthquake-induced vibrations in high-rise buildings. Passive, semi-active, and hybrid control systems were considered, including tuned mass dampers (TMDs), multiple tuned mass dampers (MTMDs), tuned liquid dampers (TLDs), inerter-based, viscous, viscoelastic, and magnetorheological dampers. Based on studies published between 2000 and 2025, the authors compared the effectiveness, optimization methods, and application characteristics of these damping systems. The analysis demonstrated that passive systems can reduce the dynamic response by up to 40–60%, while MTMDs and inerter-based devices provide enhanced robustness against detuning. Semi-active and hybrid systems offer additional advantages owing to their adaptive control capabilities.

Kim et al. [28] investigated the effectiveness of hybrid buckling-restrained braces (H-BRBs), which combine buckling-restrained braces (BRBs) with viscoelastic dampers, in mitigating wind-induced vibrations of high-rise buildings. A comparative analysis of structural systems equipped with conventional steel braces, BRBs, and H-BRBs was conducted using a 40-story steel building subjected to wind loading. The results demonstrated that the H-BRB system increases the lateral stiffness and reduces the dynamic response of the building, with the most effective vibration mitigation achieved when the dampers are installed on the lower stories.

Zhong et al. [29] reviewed modern approaches to mitigating wind-induced vibrations in super-tall buildings, including passive, active, and semi-active control strategies, aerodynamic optimization, and methods for dynamic response analysis. Particular attention was given to tuned mass dampers (TMDs), tuned liquid dampers (TLDs), hybrid damping systems, and inerter-based dampers. The study identified hybrid systems, intelligent control technologies, and integrated aerodynamic optimization of high-rise buildings as promising directions for further development.

Zhao et al. [30] investigated wind-induced vibrations of high-rise structures in the along-wind, cross-wind, and torsional directions using a two-way fluid–structure interaction (FSI) approach. Numerical simulations were performed using CalculiX, OpenFOAM, and preCICE. The results showed that accounting for coupled vibrations significantly affects the dynamic response of the structure: along-wind displacements increased by approximately 300%, while cross-wind displacements decreased by 20%, and the correlation between along-wind and cross-wind vibrations under vortex-induced resonance reached 0.8. These findings highlight the importance of considering three-dimensional aerodynamic interactions in the wind-resistant design and analysis of high-rise structures.

El Ouni et al. [31] presented a review of vibration control strategies for high-rise buildings subjected to seismic and wind loads, with particular emphasis on their practical applications. Various damping systems were examined in terms of their effectiveness, cost, installation complexity, and maintenance requirements. Tuned mass dampers (TMDs), tuned liquid dampers (TLDs), and bracing systems have found the most widespread practical application due to their effectiveness and operational feasibility. Semi-active and active control systems were identified as promising directions for future development, particularly in conjunction with the advancement and implementation of modern digital technologies.

Kang et al. [32] investigated the effectiveness of negative-stiffness inerter-based dampers for protecting adjacent buildings against seismic excitations and preventing structural pounding. A dynamic model of the coupled structural system was developed, and the optimal damper parameters were determined using the H_2-norm theory and the Monte Carlo pattern search method. The results demonstrated that the proposed devices reduce inter-story drifts and the risk of pounding between adjacent buildings, while enhancing the seismic performance and overall stability of the structural system.

Mirsaidov et al. [33–35] investigated the dynamics of various axisymmetric structures, accounting for the nonlinear elastic and viscoelastic properties of the material. The natural frequencies and decrements of vibration of the structures under steady-state kinematic loads were determined.

The analysis of scientific research indicates that current methods for calculating and designing systems with dynamic vibration dampers are highly effective and widely used to mitigate dynamic impacts on engineering structures. However, there are still challenges to be addressed, such as optimally selecting the parameters of dynamic vibration dampers, accounting for the nonlinear properties of materials, enhancing the accuracy of mathematical modeling, and developing effective methods for analyzing complex spatial systems.

2. Mathematical model

Let us consider a high-rise axisymmetric structure of annular cross-section F(z) with a piecewise constant slope of the generatrix, at different elevations of which viscoelastic dynamic vibration dampers (VDVD) are installed .

The upper part (z = H) of the structure is free. The lower part (z = 0) is on a rigid foundation, subject to a periodic kinematic action $w_0(0,t)$. It is assumed that the material of the structure possesses elastic and viscoelastic properties.

2.1. Natural oscillations of high-rise structures

It is necessary to investigate free vibrations of the structure in the absence of external excitations and without dynamic vibration dampers in the system under study (**Figure 1**).

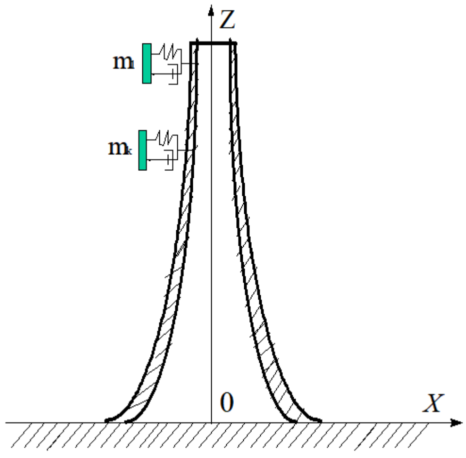

Figure 1. Model of a high-rise axisymmetric structure with DVD.

The dynamic behavior of the structural system shown in **Figure 1** is formulated by applying the principle of virtual displacements in conjunction with d'Alembert's principle

$$\delta A_m + \delta A_u + \delta A_g + \delta A_{gg} = 0 \tag{1}$$

Kinematic boundary conditions are:

$$z = 0 : w = 0; \frac{dw}{dz} = 0. \tag{2}$$

Here:

δA_m, δA_u the first term represents the virtual work associated with the structural bending moments and inertia forces;

δA_g, δA_{gg} the second term corresponds to the virtual work produced by the inertia forces of the attached masses together with the elastic and viscoelastic components of the DVD.

The specified work is calculated as:

$$\begin{gathered} \delta A_m = -\int_0^H \widetilde{M}_z \delta\left(\frac{\partial^2 w}{\partial z^2}\right) dz; \quad \delta A_u = -\rho\int_0^H F(z)\left(\frac{\partial^2 w}{\partial t^2}\right)\delta w dz; \\ \delta A_g = -\sum_{k=1}^N m_k \ddot{w}_k \delta w_k; \delta A_{gg} = -\sum_{k,l=1}^N \widetilde{K}_{kl} w_k \delta w_l \end{gathered} \tag{3}$$

In the above expressions, $\widetilde{M}_Z$ denotes the bending moment, while $w(z, t)$ represents the transverse displacement of the neutral axis at the coordinate (z). The parameter ρ is the density of the structural material. The quantities J(z), F(z), D, d and H correspond to the cross-sectional moment of inertia, cross-sectional area, external diameter, internal diameter, and structural height, respectively. The parameters m_k denote the masses attached to the dampers, and (N) is the total number of attached masses.

If the structure material has viscoelastic properties, then the relationship between stresses and strains is described by the Boltzmann–Volterra hereditary theory [36,37]:

$$\widetilde{\sigma}_z = E[\varepsilon_z - \int_0^t R_1(t-\tau)\varepsilon_z(\tau)dz] \tag{4}$$

In this case, the relationship between beam deflection w and deformation ε_z is calculated by the following formula:

$$\varepsilon_z = -x\frac{\partial^2 w}{\partial z^2}, \tag{5}$$

the relationship between bending moment $\widetilde{M}_z$ and stress $\widetilde{\sigma}_z$ has the following form:

$$\widetilde{M}_z = \int_F x\widetilde{\sigma}_z dF, \tag{6}$$

where F(z) is the cross-sectional area of the beam.

The damper spring also has viscoelastic properties, i.e.,

$$\widetilde{K}_{ki} = K_{ki}[\phi_2(t) - \int_0^t R_2(t-\tau)\phi_2(\tau)d\tau]. \tag{7}$$

Here: $\widetilde{K}_{ki}$ is the long-term stiffness of the damper; K_{ki} is the instantaneous stiffness of the damper spring; R_1 and R_2 are the relaxation kernels of the viscoelastic material of the structure and the DVD spring.

To account for the dissipative properties of the structural material and the damper spring, the Boltzmann–Volterra hereditary theory is employed in Equations (4) and (7), since this theory takes into account both stress relaxation and creep phenomena in the material.

Equations (1) and (3)–(7) and kinematic boundary conditions of Equation (2) enter the statement of the problem.

Natural oscillations of a structure are ordered movements of a structure that occur in the absence of external influences.

In the analysis of the free vibrations of the structure (without the DVD), i.e., within the framework of the governing Equations (1) and (3)–(7) and the boundary conditions of Equation (2), terms δA_g and δA_{gg} are neglected. The nontrivial solution of the variational Equation (1) is sought in the following form:

$$w(x,t) = w^*(z)e^{-iwt} \tag{8}$$

Here: w^* is the parameters that represent the natural frequencies and mode shapes of the structure (**Figure 1**).

The finite element method (FEM) is employed to transform the original variational formulation into a complex algebraic eigenvalue problem of the following form:

$$([\overline{K}] - \omega^2[M])\{x\} = 0 \tag{9}$$

$[\overline{K}]$ is the complex stiffness matrix of a structure depending on ω_R;

$[M]$ is the mass matrix of a structure;

$\omega = \omega_R - i\omega_I, \{x\} = \{x_R\} - i\{x_I\}$ are the complex natural frequencies and vectors, respectively.

The structure is discretized using truncated conical finite elements [31], in which the displacement field is represented by cubic interpolation functions.

In this case, assuming that the terms in the integral Equations (4) and (7) are small, the long-term elasticity moduli and stiffness of the damper spring are approximately replaced by the following relation [36,37]:

$$\widetilde{E} \approx \bar{E} = E\left[1 - i\Gamma_1^s(\omega_R) - \Gamma_1^c(\omega_R)\right], \tag{10}$$

$$\widetilde{K}_{ki} \approx K_{ki}\left[1 - ii\Gamma_2^s(\omega_R) - \Gamma_2^c(\omega_R)\right], \tag{11}$$

where E is the instantaneous modulus of elasticity of the material; K_{ki} is the instantaneous stiffness of the DVD spring;

$$\Gamma_1{}^C(\omega_R) = \int_0^\infty R_1(t)\cos(\omega_R\tau)d\tau, \Gamma_1{}^S(\omega_R) = \int_0^\infty R_1(t)\sin(\omega_R\tau)d\tau,$$

$$\Gamma_2{}^C(\omega_R) = \int_0^\infty R_2(t)\cos(\omega_R\tau)d\tau, \Gamma_2{}^S(\omega_R) = \int_0^\infty R_2(t)\sin(\omega_R\tau)d\tau.$$

The functions $R_1(t)$, $R_2(t)$ represent the cosine and sine Fourier transforms of the relaxation kernels.

Thus, the considered variational problem defined by Equations (1) and (3)–(7) is reduced to the determination of complex natural frequencies $\omega = \omega_R - i\omega_I$ and complex mode shapes $w^*(z)$ that satisfy Equation (1) with the corresponding kinematic conditions of Equation (2) for any admissible displacement field δw^*.

From Equation (9), the complex natural frequencies of the problem are determined by the Muller method [38] and the natural modes of oscillations by the Gauss method [39].

2.2. Steady-state forced oscillations of the "high-rise structure–dynamic vibration damper" system

Steady-state forced oscillations of the system occur in the presence of external periodic effects. In this case, the initial conditions are not considered.

As a kinematic excitation applied to the foundation of the structure, a periodic disturbance is considered, described by the following expression:

$$z = 0 : w_0(0, t) = \phi(t). \tag{12}$$

In the problem of steady-state forced oscillations of the "high-rise structure–dynamic vibration damper" system, it is necessary to determine the displacement field in the system under consideration that satisfies Equations (1) and (3)–(7), kinematic boundary conditions of Equation (2), and periodicity conditions for any virtual displacement δw.

The solution to the variational problem under consideration is sought in the following form:

$$w(z,t) = w_0(t) + w^*(z)e^{-ipt} \tag{13}$$

$w^* = w_R^* - iw_i^*$ is the sought-for complex amplitude; p is the given actual frequency of the external effect; $w_0(t)$ is the given kinematic effect.

By employing the finite element method (FEM) and discretizing the structure using truncated cone finite elements [35], the considered problem is reduced to a large-scale system of algebraic equations with complex coefficients of the following form:

$$([\bar{K}] - p^2[M])\{x\} = \{f\} \tag{14}$$

In solving the problem of steady-state forced vibrations, the parameters in Equations (4) and (7) are replaced by the following exact expressions [36, 37], since in this case the lower limits of the integrals in Equations (4) and (7) are taken to be minus infinity:

$$\widetilde{E} \cong \bar{E} = E\left[1 - i\Gamma_1^s(p) - \Gamma_1^c(p)\right], \tag{15}$$

$$\widetilde{K} \cong \bar{K} = K\left[1 - i\Gamma_2^s(p) - \Gamma_2^c(p)\right], \tag{16}$$

where Γ_1^s, Γ_1^c, Γ_2^s, Γ_2^c are the sine and cosine Fourier images of relaxation kernels R_1 and R_2, respectively.

Here, $\left[\overline{\mathrm{K}}\right]$ is the complex stiffness matrix, and [M] is the mass matrix of the structure equipped with a DVD; $\{f\}$, $\{x\}$ denote the amplitude vector of the external excitation and the unknown complex displacement vector, respectively.

The complex system of algebraic Equation (14) is then solved using the Gaussian elimination method for different prescribed values of the external excitation frequency "p".

2.3. Unsteady forced vibrations of the "high-rise structure–dynamic vibration damper" system

Unsteady forced vibrations of the "high-rise structure – dynamic vibration damper" (HRS-DVD) system occur due to short-term non-periodic impacts; they substantially depend on the initial configuration and velocity of impact.

In problems of unsteady forced vibrations of the HRS-DVD system for given function $w_0(t)$ with initial conditions u_0, v_0, it is necessary to find deflection w(z,t), strains $\varepsilon_z(z,t)$, stresses $\sigma_z(z,t)$, satisfying Equations (1) and (3)–(7) with given kinematic conditions of Equation (2) and initial conditions ($t = 0$: $w(z,0) = u_0$: $w(z,0) = v_0$) for any virtual δw.

The solution of the formulated variational problem is expressed in the following form:

$$w(z,t) = w_0(t) + w^*(z,t), \tag{17}$$

where $w^*(z,t)$ is the sought-for amplitude of displacements.

Using the FEM procedure with discretization of the structure by a finite element in the form of a truncated cone [31], we reduce the variational problem under consideration to a system of nonlinear integro-differential equations of the following form:

$$\begin{gathered}[M]\{\ddot{w}(t)\} + [K]\{w(t)\} = \{P(t)\} + \int_0^t R_1(t-\tau)[K_1]\{w_1(\tau)\}d\tau + \\ \int_0^t R_2(t-\tau)[K_2]\{w_2(\tau)\}d\tau,\end{gathered} \tag{18}$$

with initial conditions

$$t = o : \begin{matrix} w(z,0) = u_0 \\ \dot{w}(z,0) = v_0 \end{matrix}, \tag{19}$$

where u_0 and v_0 are the given values.

The following notations are used in the system of integro-differential Equation (18): [K] and [M] are the stiffness and mass matrices of the structure with the DVD, respectively; $[K_1]$ is the stiffness matrix of the structure; $[K_2]$ is the stiffness matrix of the DVD; R_1 is the relaxation kernel for the viscosity of the structure material; R_2 is the relaxation kernel for the damper spring; $\{w_2(t)\}$ is the displacement components of the DVD at the specified points on the structure; $\{w\} = \{w_1\} + \{w_2\}$ is the displacement vector of various points of the structure and the DVD.

The system of integro-differential Equation (18), together with the initial conditions specified in Equation (19), is solved numerically by means of the Newmark integration algorithm [40].

A feature of the algorithm for solving Equation (18) is that the integrals entering Equation (18) are calculated from the beginning of the process, while at each step, the integrals are determined within the limits from t_i to t_{i+1}. In this case, the full value of the integral at time t_{i+1} is obtained by summing the value saved at the previous step with the integral obtained at the last stage, with integration limits from t_i to t_{i+1}.

To implement all the tasks outlined in this article, special algorithms and a program for an IBM PC using complex arithmetic were developed.

3. Results and discussion

The natural vibrations of a structure without a DVD, and steady-state and unsteady forced vibrations of high-rise axisymmetric structures with dynamic vibration dampers under various impacts were studied. As an example of calculation, the Novo-Angren high-rise smokestack was considered using actual geometric dimensions (height H = 330 m) and real physical and mechanical characteristics of the material. In this case, the structure's diameter at the lower base was D = 38.0 m, and height H = 330 m, D = 16.50 m. Physical and mechanical characteristics of the materials were $E = 2.9 \times 10^4$ MPa; $\nu = 0.17$; $\rho = 2.5$ t/m^3.

3.1. Natural oscillations

Using the above methodology and calculation program, the natural frequencies and oscillation modes were determined for the elastic statement of the structure (**Figure 1**) without DVD (**Table 1**).

Table 1. Natural frequencies corresponding to the bending, longitudinal, and torsional vibration modes of the elastic structure.

No. of natural frequencies	Bending	Longitudinal	Torsional
ω_1	1.9246	28.9589	18.9309
ω_2	6.8944	47.4113	30.9937
ω_3	16.3258	83.4104	54.5271
ω_4	30.6408	119.9753	78.4303
ω_5	49.2861	138.8048	90.7904

Subsequently, the free vibrations of the structure are analyzed considering the viscoelastic properties of the structural material and neglecting the effects of the DVD.

The Rzhanitsyn-Koltunov kernel [33–35] was used as the relaxation kernel:

$$R(t) = Ae^{-\beta t}t^{\alpha-1} \tag{20}$$

The kernel parameters A, β, α were determined using the M.A. Koltunov method [36, 37] from experimental creep curves of concrete: $A = 0.0194$; $\beta = 0.00000014$; $\alpha = 0.075$.

Table 2 shows the natural frequencies of the spatial natural vibration modes of structures without a dynamic vibration damper, taking into account the viscoelastic properties of the material, obtained using the developed method and program.

Table 2. The real components of the eigenfrequencies corresponding to the bending vibration modes of the structure.

No. of natural frequencies	Bending	Longitudinal
ω_1	1.8668	28.0029
ω_2	6.6876	45.8467
ω_3	15.8360	80.6576
ω_4	29.6297	119.9753
ω_5	47.6597	134.2242

The results show that the developed method is suitable for solving the problem of natural vibrations of high-rise structures, considering the elastic and viscoelastic properties of the structure's material.

Analysis of the natural frequencies presented in **Tables 1** and **2** revealed the values entering the range of dominant frequencies of seismic impacts (2–10 Hz). This fact indicates a potential risk of a dangerous resonance regime in the considered high-rise structure during an earthquake. This, in turn, necessitates a more detailed dynamic analysis taking into account the spectral characteristics of seismic excitation and the damping properties of the HRS-DVD system.

To verify the reliability of the obtained results and further develop our research, the natural vibrations of the Novo-Angren high-rise smokestack were studied using the ANSYS and ABAQUS software tools, which are among the most modern software available today.

When comparing the results presented in **Tables 1–3**, it can be seen that the results we obtained are close to the results obtained using the software.

Table 3. Natural frequencies of the Novo-Angren high-rise smokestack.

No.	No. of natural frequencies	ANSYS	ABAQUS
1.	ω_1	1.889	1.769
2.	ω_2	1.890	1.770
3.	ω_3	6.744	6.235
4.	ω_4	6.772	6.237
5.	ω_5	15.064	14.487
6.	ω_6	15.149	14.693
7.	ω_7	16.324	15.773
8.	ω_8	16.372	15.812
9.	ω_9	19.692	19.092
10.	ω_{10}	22.283	21.684
11.	ω_{11}	22.425	21.879
12.	ω_{12}	23.737	22.948

3.2. Steady-state forced vibrations

Steady-state forced vibrations of high-rise structures with dynamic vibration dampers located at different levels were studied (**Figure 1**).

In dynamic calculations, a kinematic harmonic impact was applied to the base of the structure

$$z = 0{:}w_0(t) = Be^{-ipt}, \tag{21}$$

where B, p are the amplitude and frequency of the external impact.

To assess the efficiency of damping the structure vibrations, the values of the maximum amplitudes of displacements of some points of the structure are studied at different frequencies of external impact p.

The amplitude-frequency responses (AFR) were constructed for each of the considered points of the structure, i.e., z = 20.0 m, z = 60.0 m, z = 95.0 m, z = 120.0 m, z = 145.0 m, z = 195.0 m, z = 230.0 m, z = 245.0 m, z = 270.0 m, z = 290.0 m, z = 325.0 m, considering the dissipative properties of the structure material and DVD.

In the calculations, the frequency response results for structures with a DVD are given for three values of the damper spring stiffness, i.e., three values of stiffness K_{11} were selected: the first stiffness was less than the one close to the first natural oscillation frequency ω_1, the second—between the first and second frequencies, and the third—close to the second natural oscillation frequency ω_2 [35].

The steady-state forced oscillations of a structure with a damper were studied for various parameters of the system:

1. The structure material has weak viscoelastic properties, and the damper is elastic;
2. The structure material is elastic, and the damper is viscoelastic;
3. The structure material has weak viscoelastic properties, and the damper is viscoelastic.

3.2.1. Steady-state oscillations of a viscoelastic structure with an elastic spring

Steady-state oscillations of a viscoelastic structure with an elastic spring are studied to determine the amplitude-frequency response. **Figure 2** shows the frequency response for different points (z = 290 m; z = 325 m) of the viscoelastic structure (A = 0.00194; $\alpha = 0.075$; $\beta = 0.00000014$) with an elastic spring of different damper stiffness $K_{11} = 2.85$ (a solid line). The damper mass is $m_1 = 0.0004$ M.

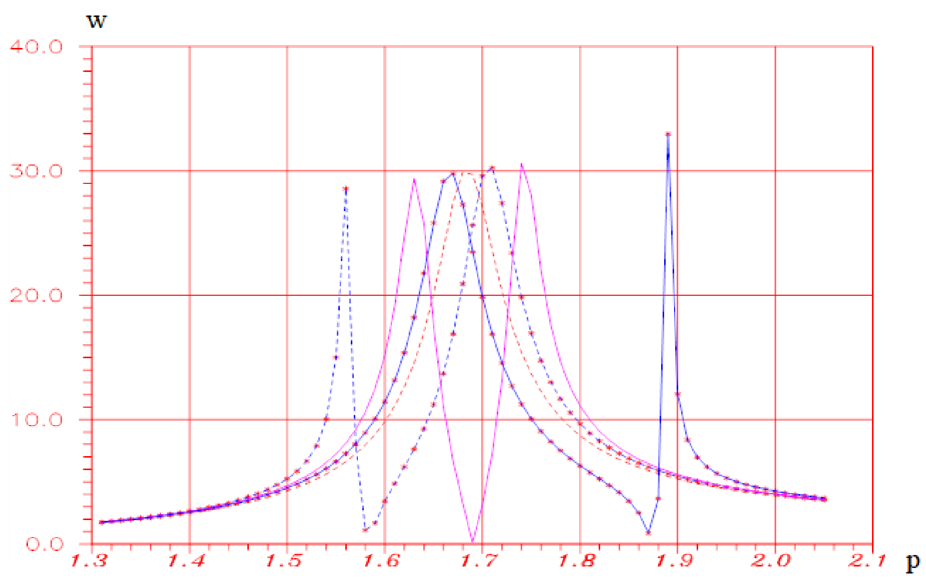

Point at z = 290 m

Figure 2. *Cont.*

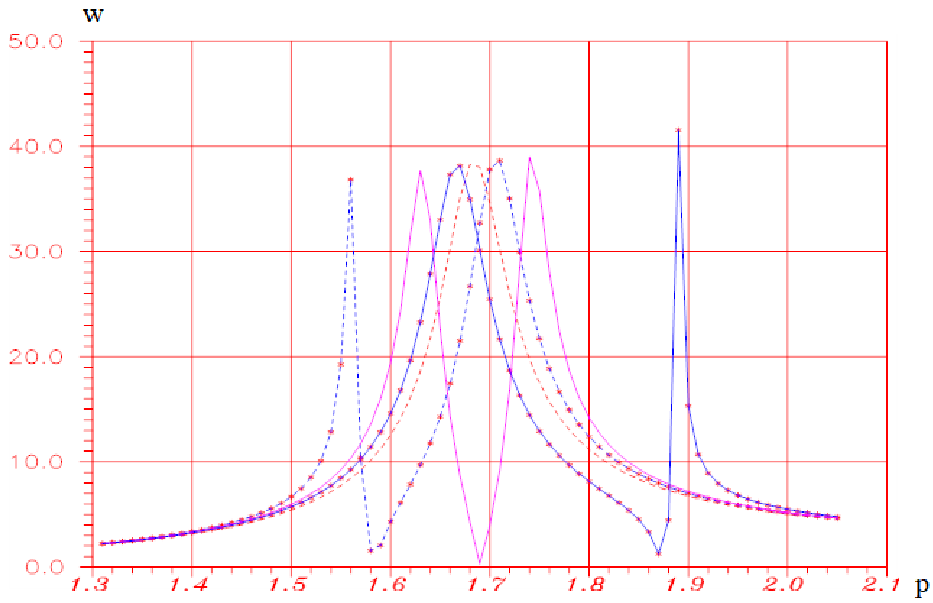

Figure 2. Frequency response for different points of a viscoelastic structure with an elastic DVD of mass $m_1 = 0.0004$ M.

As shown in **Figure 2**, the red dashed curve represents the structure without DVD. The blue dashed curve with asterisks show the frequency response of the viscoelastic structure with the elastic damper stiffness $K_{11} = 2.5$; the magenta solid curve was obtained for $K_{11} = 2.85$; and the blue solid curve with asterisks was obtained for $K_{11} = 3.5$ [35]. For comparison, the dotted line shows the solution obtained for the same points (z = 290 m; z = 325 m) of a viscoelastic structure without a DVD.

In all graphs presented (**Figure 2**) for a structure with a DVD, two resonance peaks are obtained, one of which represents the amplitude of the structure's oscillations when the impact frequency p is close to the structure's natural frequency, and the other represents the amplitude of the structure's oscillations when the impact frequency p is close to the damper's natural frequency. From a comparison of the frequency responses obtained for a structure without a DVD and with a DVD, it is clear that the vibration amplitudes of the structure with an elastic DVD do not decrease. Moreover, in the presence of a DVD, instead of one resonant peak, two peaks are observed, one of which shifts either to the left or to the right depending on the frequency of natural oscillations of the DVD.

It should be noted that for a spring stiffness of $K_{11} = 2.5$, there is a very insignificant transfer of dissipative properties from the structure to the DVD; the DVD behaves almost elastically and the structure behaves viscoelastically. For $K_{11} = 2.85$, there is a sufficient transfer of dissipative properties from the structure to the damper; therefore, the structure and the damper behave viscoelastically.

For $K_{11} = 3.5$, a significant transfer of dissipative properties occurs from the structure to the damper, resulting in the damper behaving viscoelastically and the structure behaving elastically. In this case, the viscoelastic structure dampens the oscillations of the elastic damper. If these results are compared with those of the vibrations of the structure without a DVD, the maximum amplitudes of vibrations of the structure with a DVD remain unchanged in magnitude. Thus, in this case, the DVD does not provide the effect of damping the vibrations of the structure.

3.2.2. Steady-state vibrations of an elastic structure with a viscoelastic spring

Steady-state vibrations of an elastic structure with a viscoelastic spring are studied to determine the amplitude-frequency response. **Figure 3** shows the frequency response for the most characteristic points (z = 290 m; z = 325 m) of an elastic structure with a viscoelastic damper spring ($\Gamma_2^c = 0.2$; $\Gamma_2^s = 0.02$). The following values of damper spring stiffness are taken for the calculation: the dashed curve represents the structure without DVD; the dashed curve with asterisks represents $K_{11} = 4.0$ (when $\omega_{I1} < \omega_{I2}$); the solid curve is for $K_{11} = 4.6$ (when $\omega_{I1} \approx \omega_{I2}$); the solid curve with asterisks shows $K_{11} = 5.5$ (when $\omega_{I1} > \omega_{I2}$). The stiffness values are taken from the results obtained by the authors [31].

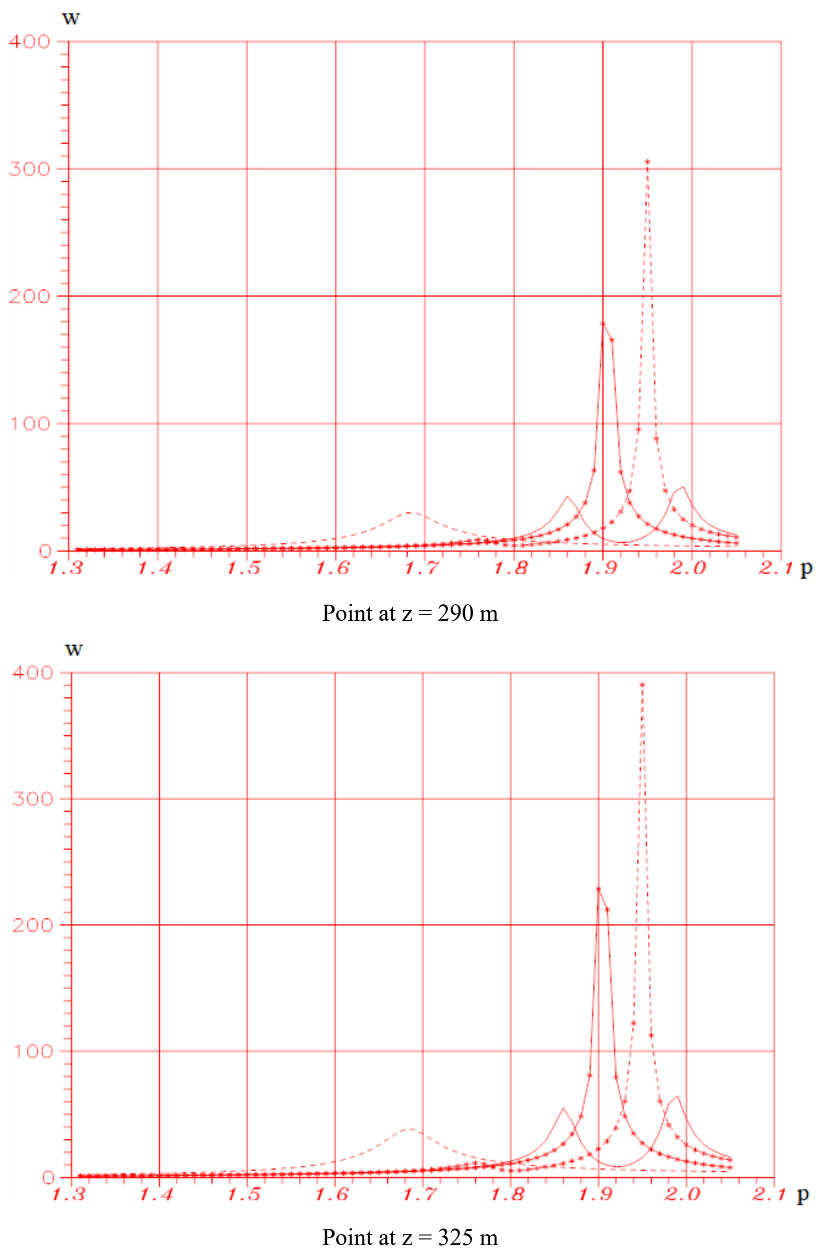

Figure 3. Amplitude-frequency response for different points of an elastic structure with a viscoelastic DVD ($\Gamma_2^c = 0.2$; $\Gamma_2^s = 0.02$) of mass $m_1 = 0.0004$ M.

For comparison, the frequency response for a viscoelastic structure without a damper is shown by the dotted line. As is known, if the structure is elastic and without a damper, the amplitude of the structure's oscillations at resonance would be infinite.

If we analyze the results, we can see that at $K_{11} = 4.0$, the amplitude of the structure's oscillations at resonance (when the frequency of the external action p is close to the structure's natural frequency ω) is high and several times exceeds the amplitude of the oscillations of a viscoelastic structure without a damper; the first resonant peak (when p ≈ ω, the damper's natural frequency) is almost imperceptible, i.e., at $K_{11} = 4.0$, the transfer of dissipative properties from the damper to the structure almost does not occur.

If the spring stiffness is $K_{11} = 4.6$, then two almost identical resonant peaks appear on the amplitude-frequency response (the first of which corresponds to the damper's oscillation frequency, and the second to the structure's oscillation frequency). The amplitude of these two peaks is greater than the amplitude of the oscillations of a viscoelastic structure without a damper. In this case, sufficient dissipation transfer from the damper to the structure occurs.

In the third case, at $K_{11} = 5.5$, the first resonant peak is quite large—this corresponds to the resonance of the structure (when p ≈ ω—the natural frequency of the damper), which behaves elastically at these frequencies. The second peak corresponds to the resonance of the structure (when p ≈ ω—the natural frequency of the structure). The structure behaves viscoelastically, and all dissipation is transferred from the damper to the structure.

The greatest effect of vibration damping was observed only in the third case. Therefore, steady-state forced vibrations of a viscoelastic structure with a damper containing a viscoelastic damping element installed in it are considered below for different values of the spring stiffness.

3.2.3. Steady-state vibrations of a viscoelastic structure with a viscoelastic damper spring of different stiffness

Steady-state vibrations of a viscoelastic structure with a damper as a viscoelastic spring of varying stiffness are studied to determine the amplitude-frequency response.

Figure 4 shows the change in the amplitude-frequency responses for points at the height 325 m of the viscoelastic structure when installing a viscoelastic DVD with mass $m_1 = 0.0004$ M at different values of the damper spring stiffness, i.e., at $K_{11} = 3.25$; 3.35; 3.45; 3.55; 3.65; 3.75.

These calculations used viscoelastic parameters with the following values [32]: for the structure material A = 0.00194; α = 0.075; β = 0.00000014 and for the viscoelastic damper spring $\Gamma_2 = 0.2$; $\Gamma_2^s = 0.02$. The mass of the damper was taken as $m_1 = 0.0004$ M (M is the mass of the structure).

The frequency response of a structure with a DVD is shown in all graphs by a solid line. The frequency response of a viscoelastic structure without a damper is shown by a dotted line.

As seen from the results in **Figure 4**, obtained for the point of the structure z = 325 m at different values of the spring stiffness K_{11}, i.e., $K_{11} < K_{11}^*$ (K_{11}^* is the spring stiffness that ensures the frequency of the spring equal to the first natural frequency of the structure, i.e., $\omega_{\text{п}} \approx \omega_{\text{г}}$), the first amplitude peak (resonance occurring when the natural frequency of the damper is $\omega_1 \approx p$) is less than the second peak (resonance occurring when the natural frequency of the structure is $\omega_1 \approx p$).

As the stiffness K_{11} increases (to the value $K_{11} \approx K_{11}^*$), these peaks align, and the dissipation transfers from the larger peak to the smaller one (**Figure 4d**). According to **Figure 4a**, the oscillation amplitude of the structure at point z = 325 m with $K_{11} = 3.25$ is 38 cm. After installing the tuned mass damper, two peaks are formed at 14 cm and 32 cm. Furthermore, as the stiffness of the damper's spring increases (**Figure 4b,c**), the two peaks move closer together.

Analysis of graphs in **Figure 4d–f** shows that at $K_{11} = 3.55$, an equal reduction of both peaks was achieved, resulting in two peaks of 23 cm each (**Figure 4d**). At $K_{11} \approx K_{11}^* \approx 3.55$ both peaks have almost the same amplitude, and the highest damping of vibrations occurs. This stiffness value corresponds to the optimal parameter of the DVD.

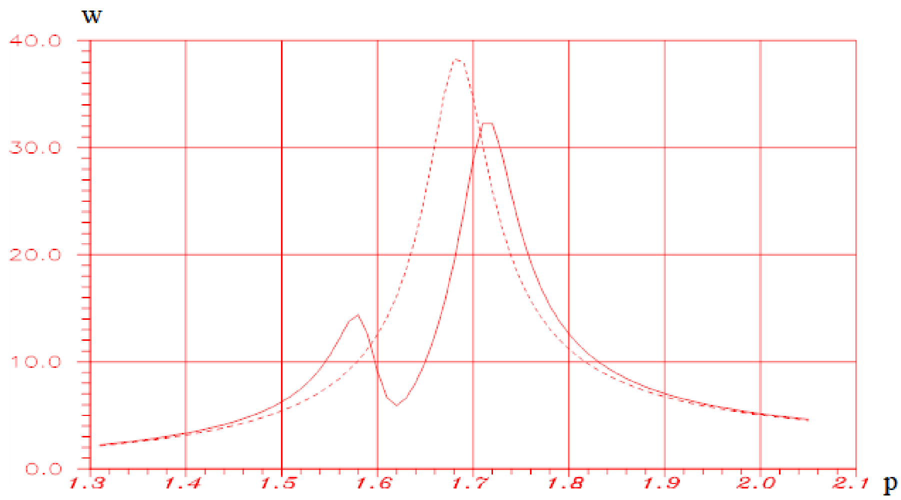

(a) $K_{11} = 3.25$

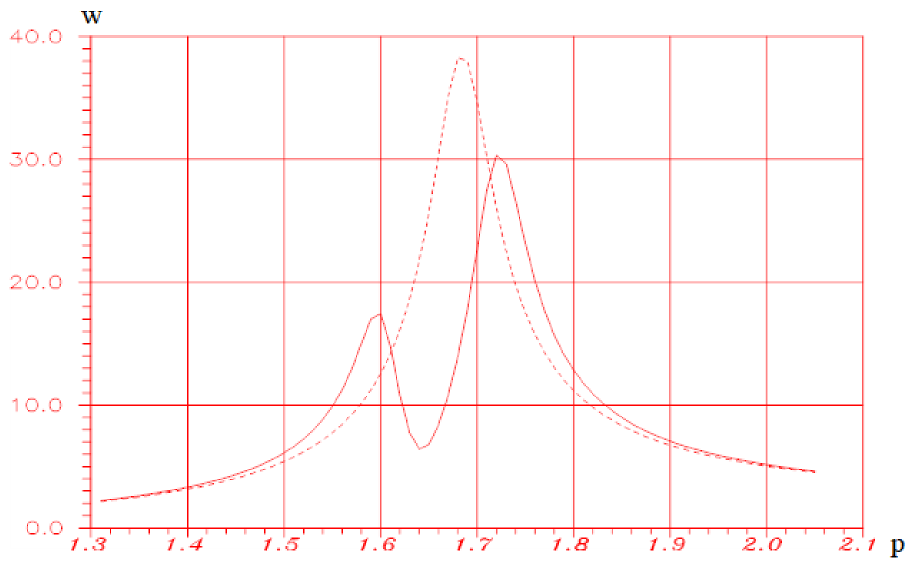

(b) $K_{11} = 3.35$

Figure 4. *Cont.*

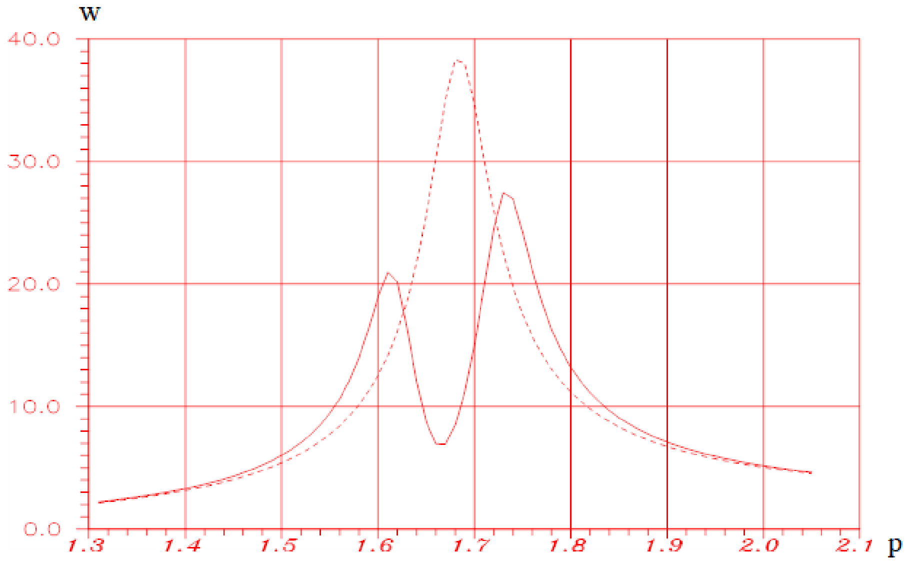

(c) K_{11} = 3.45

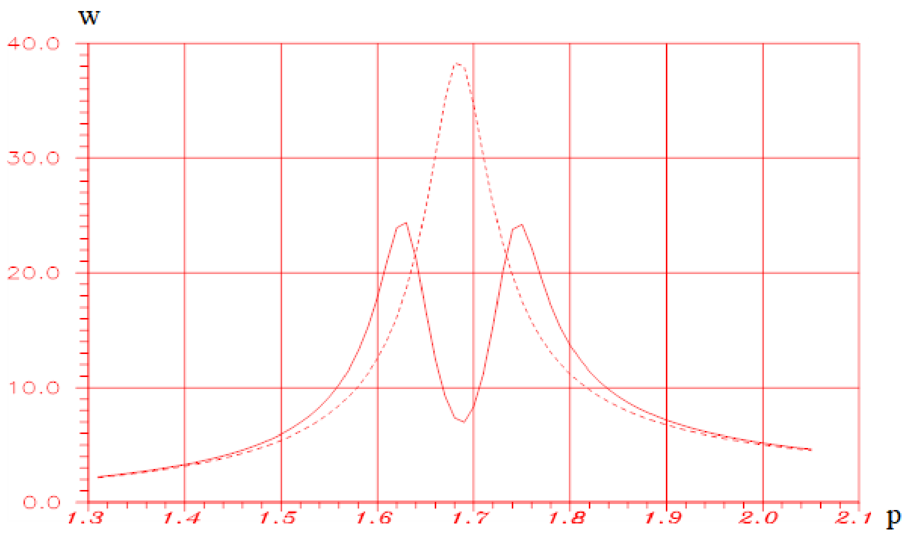

(d) K_{11} = 3.55

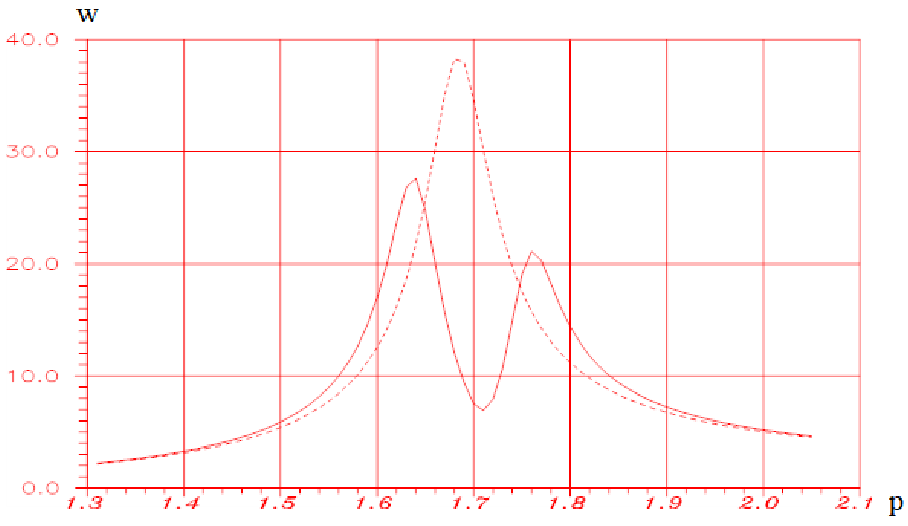

(e) K_{11} = 3.65

Figure 4. *Cont.*

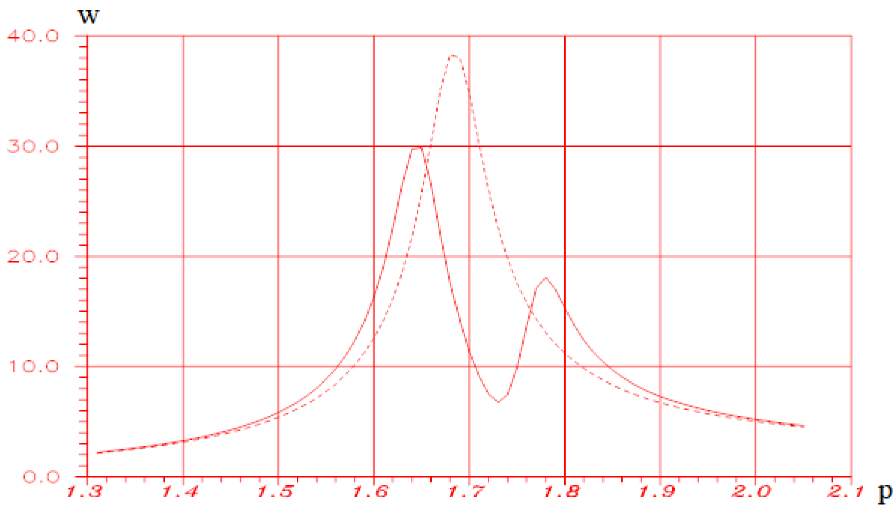

(f) $K_{11} = 3.75$

Figure 4. Change in the amplitude-frequency response for points (z = 325 m) of a viscoelastic structure with a VDVD of mass $m_1 = 0.0004$ M at different values of the damper spring stiffness.

The frequency response of a structure with a DVD is shown in all graphs by a solid curve. The frequency response of a viscoelastic structure without a damper is shown by a dotted line. Comparison of the results obtained shows that if the stiffness of the damper spring is $K_{11} \approx K_{11}{}^{*}$, the amplitude of the structure oscillations at resonance can be almost halved.

A further increase in stiffness $K_{11} > K_{11*}$ raises the amplitude of the first resonant peak, while the amplitude of the second resonant peak decreases (**Figure 4f**). This also results in undesirable consequences: the vibration damper oscillates with a high amplitude, causing the structure to oscillate at a similarly high amplitude.

Therefore, when both the structure and the spring of the dynamic vibration damper are viscoelastic but with different viscosity characteristics, it is reasonable to tune the stiffness of the dynamic damper so that their natural frequencies coincide. Tuning the dynamic vibration damper ensures the smallest amplitude of vibrations of the high-rise structure, protecting it from undesirable dynamic effects.

For the reliability of the results obtained, the amplitude-frequency responses were constructed at two levels of the structure z = 230 m and z = 290 m (**Figure 5**). When the damper is tuned optimally, i.e., at a spring stiffness of $K_{11} \approx K_{11}{}^{*}$, all points of the structure oscillate with a much smaller amplitude. Across all graphs in **Figure 5**, the solid curve depicts the frequency response of the structure with a DVD, whereas the dotted line represents the viscoelastic structure without a damper.

3.2.4. Steady-state oscillations of a viscoelastic structure with a viscoelastic spring at different values of the damper mass

The steady-state forced oscillations of a viscoelastic structure with a viscoelastic spring of the dynamic damper are investigated for different values of the damper mass. For points z = 290 m; z = 325 m of a viscoelastic structure with a viscoelastic spring of the damper (for $\Gamma_2^c = 0.2$; $\Gamma_2^s = 0.02$), the frequency responses are plotted for different values of the mass of the dynamic damper (**Figure 6**).

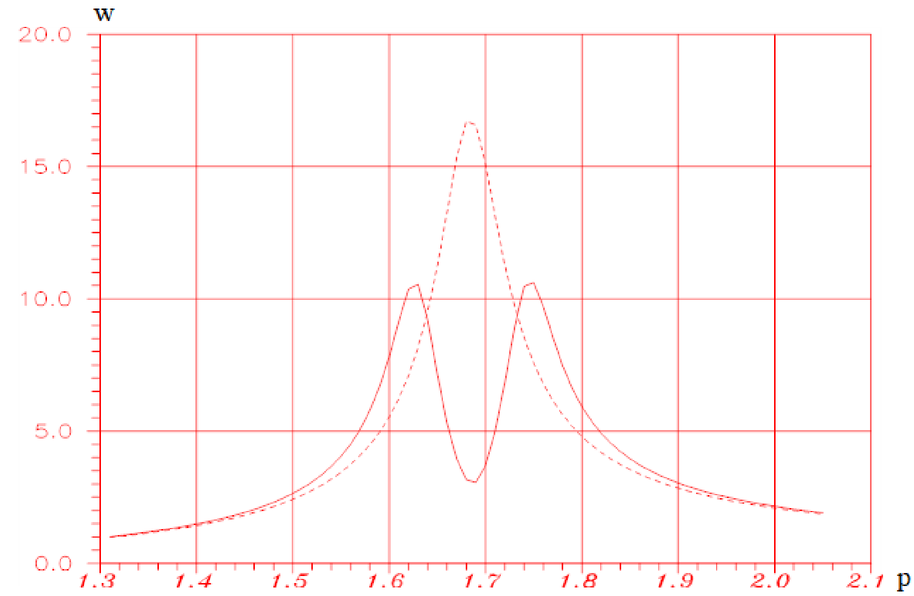

(a) Point at z = 230 m, K_{11} = 3.55

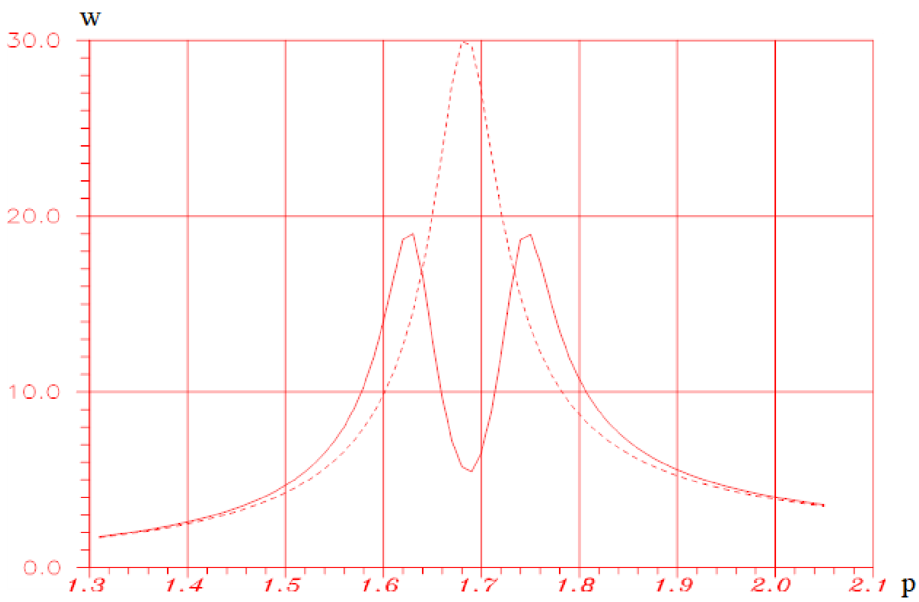

(b) Point at z = 290 m, K_{11} = 3.55

Figure 5. Amplitude-frequency response for points (z = 230 m; z = 290 m) of a viscoelastic structure with a VDVD of mass m_1 = 0.0004 M at spring stiffness value K_{11} = 3.55 of the dynamic damper.

In **Figure 6**, the dashed curve represents the system without a dynamic vibration damper (DVD). The dashed curve with asterisks corresponds to the system equipped with a damper m_1 = 0.0004 M. The solid curve with asterisks indicates the response with a damper m_1 = 0.001 M, while the solid curve denotes the case with m_1 = 0.02 M.

All the obtained results correspond to the case when the spring stiffness is $K_{11} \approx K_{11}^*$. The frequency response of a viscoelastic structure without a DVD is shown by a dotted line, a dotted line with asterisks is the case of m_1 = 0.0004 M, a solid line with asterisks is the case of m_1 = 0.001 M, and a line without asterisks is the case of m_1 = 0.02 M.

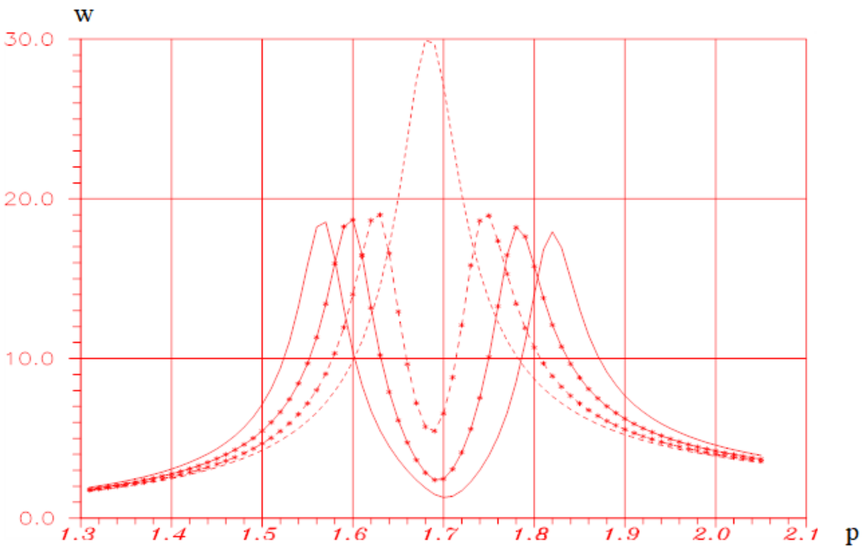

Point at z = 290 m

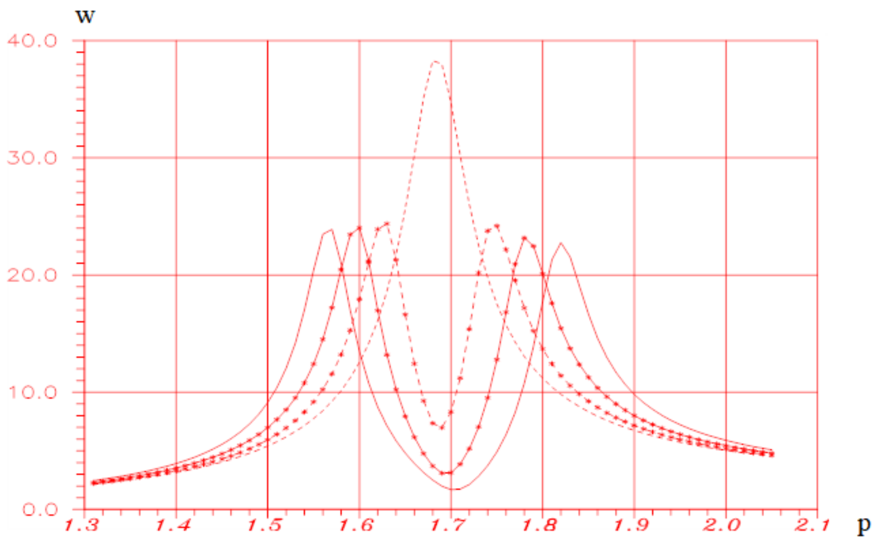

Point at z = 325 m

Figure 6. Amplitude-frequency response for different points (z = 230 m; z = 290 m; z = 325 m) of a viscoelastic structure with a VDVD at different values of the mass m_1 of the damper.

Analysis of the obtained results shows (**Figure 6**) that with an increase in the mass of the dynamic damper, the amplitude of vibrations of the structure does not decrease; this is explained by the fact that the system turns into a weakly coupled system.

A weakly coupled system is a system in which each element (i.e., a structure and a DVD) is interconnected by a weak link (i.e., a spring). During oscillation, the influence of one element on another very insignificantly alters the frequency of the system as a whole. In this case, a decrease in the DVD mass, in turn, reduces the DVD frequency, causing it to become lower than the first natural frequency of the structure. Therefore, it does not reduce the system's oscillation amplitude.

3.2.5. Effect of the viscosity of the damper spring on the steady-state vibrations of the viscoelastic structure

At the next stage, the effect of different values of the viscosity of the damper spring on the steady-state forced vibrations of the viscoelastic structure was investigated

(**Figure 7**). In the calculations, the following was assumed: the mass of the damper is $m_1 = 0.0004M$, and the stiffness of the damper spring is $K_{11} = K_{11}^*$.

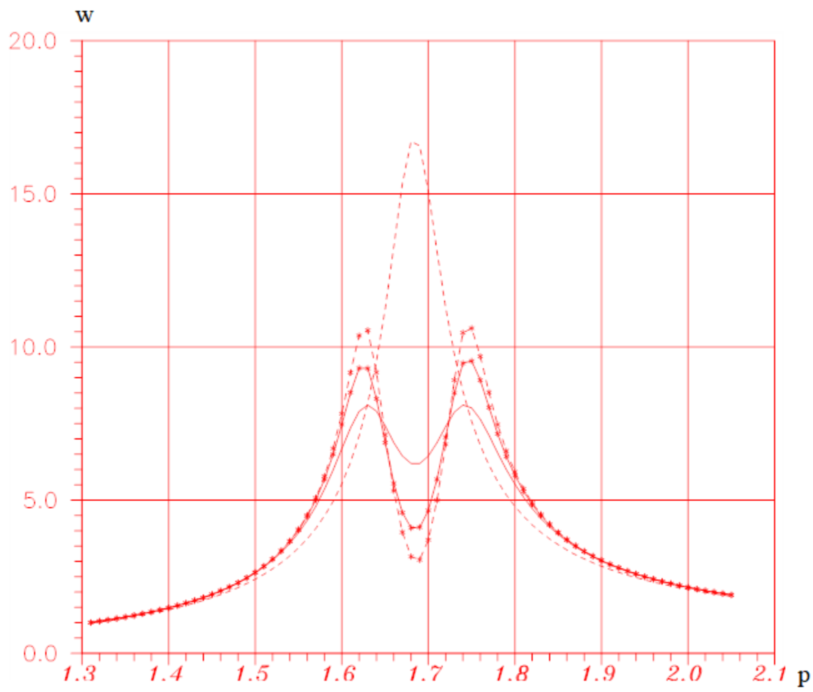

Point at z = 230 m

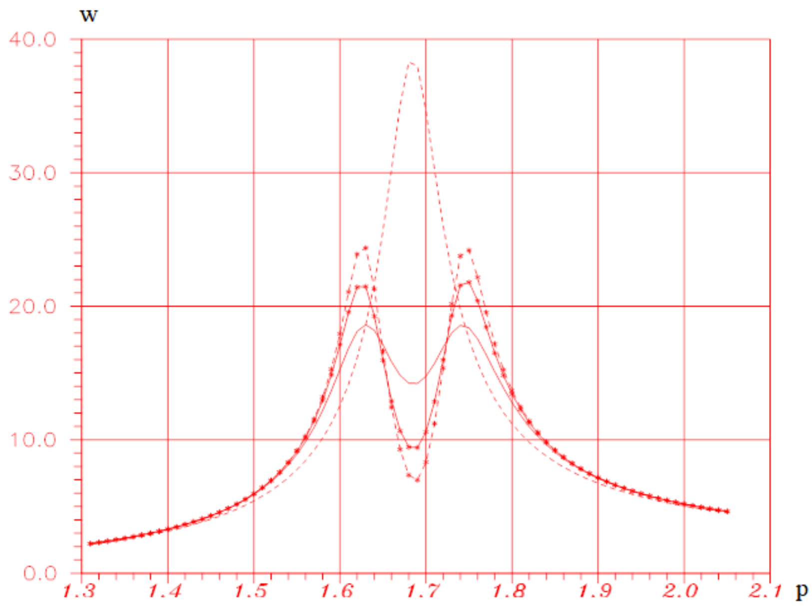

Point at z = 325 m

Figure 7. Amplitude-frequency response for different points (z = 230 m; z = 325 m) of a viscoelastic structure with a VDVD at different values of the damper spring viscosity.

As in **Figure 7**, a dotted line shows the frequency response of the viscoelastic structure without a DVD. The dotted line with asterisks corresponds to the case when the viscosity parameters of the damper are $\Gamma_2^c = 0.2$; $\Gamma_2^s = 0.02$; the solid line with asterisks corresponds to the case when the structure and the damper have the same viscosity $\Gamma_2^c = 0.28$; $\Gamma_2^s = 0.023$, (i.e., the system is homogeneous); the line without asterisks denotes the case when the damper has viscosity $\Gamma_2^c = 0.4$; $\Gamma_2^s = 0.04$.

As the stiffness K_{11} increases (to the value of $K_{11} \approx K_{11}^*$), these peaks align, and the dissipation transfers from the larger peak to the smaller one. At $K_{11} \approx K_{11}^* \approx 3.55$, both peaks have almost the same amplitude, and the greatest damping of oscillations occurs. This stiffness value corresponds to the optimal parameter of the DVD.

From the results obtained, it can be concluded that as the viscosity of the dynamic damper spring increases, the amplitude of oscillations of a high-rise structure at resonance is significantly reduced. With these parameters, a strongly intercoupled system is formed, and it is possible to dampen the amplitude of oscillations of the structure to the maximum.

3.3. Unsteady forced oscillations

Unsteady forced oscillations of high-rise axisymmetric structures with dynamic oscillation dampers are studied (**Figure 1**) to identify the possibility of reducing the amplitude of oscillations of structures under various non-stationary kinematic effects. The oscillations considered here are assumed to be short-term and substantially dependent on the initial parameters of the external impact. To assess the effectiveness of a dynamic oscillation damper, the amplitude of oscillations of a structure without a damper and with dynamic vibration dampers installed at different levels of the structure over the entire period of impact is determined.

The parameters of the relaxation kernel in the calculation were taken for the structure $A_1 = 0.0194$, $\alpha_1 = 0.075$, $\beta_1 = 14 \times 10^{-8}$, for the spring $A_2 = 0.014$, $\alpha_2 = 0.075$, $\beta_2 = 14 \times 10^{-8}$. In the calculation, the damper was installed at the mark z = 325 m. Its mass was m = 0.0004 M.

Figure 8 shows the results obtained under a long-term harmonic impact, i.e., a kinematic impact of the following form:

$$z = 0 : \ddot{u}_0 = \sin(pt) \tag{22}$$

with the impact frequency p close to the natural frequency ω_0 of the bending vibrations of the structure.

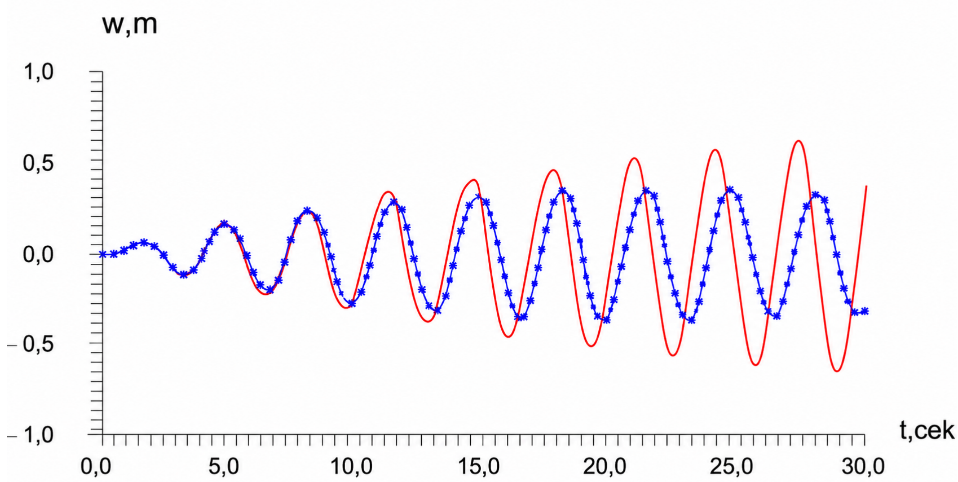

Figure 8. Change in displacement of the upper point of the structure (z = 325 m) under long-term harmonic impact with a frequency close to the frequency of natural oscillations of the HRS-DVD system: structure without DVD (red curve); structure with DVD (blue curve with asterisks).

Figure 9 shows the results obtained under a short-term harmonic of Equation (22) impact (0 < t < 6 s) with the same frequency; the solid line corresponds to the displacement response of the stack top without vibration control, while the asterisk-marked curve illustrates the response after installing the DVD.

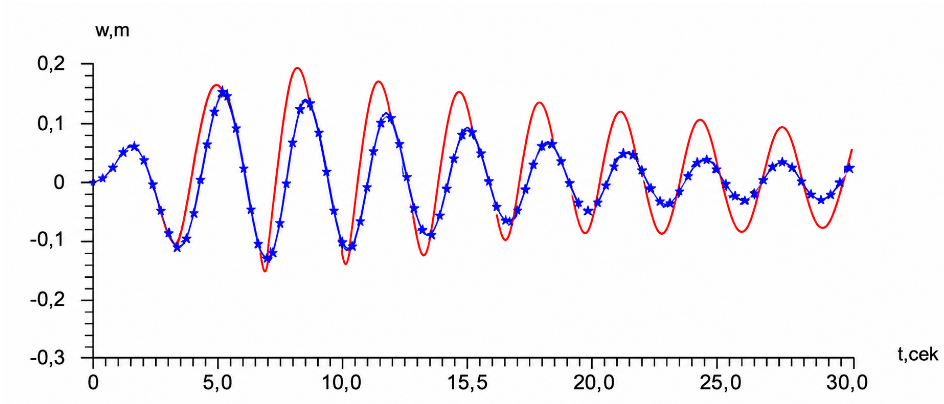

Figure 9. Change in displacement of the upper point (z = 325 m) of the structure under short-term harmonic impact (t = 6 s) with a frequency close to the frequency of natural oscillations of the HRS-DVD system: structure without DVD (red curve); structure with DVD (blue curve with five-pointed stars).

Comparison of the results in **Figures 8** and **9** shows that the DVD significantly reduces the vibration amplitude of the structure, to the frequency of which it is tuned. Thus, in **Figure 8**, under a long-term harmonic impact with a frequency close to the vibration frequency of the structure (1.75 rad/s), the amplitude of vibrations that arise in the latter increases with each period up to a certain point (a solid line).

The presence of a damper with a natural frequency of 1.884 rad/s reduces the oscillation amplitude by more than one and a half times. At a relatively short-term impact (in **Figure 9**, t = 6 s), after the effect ceases, free damped oscillations are established in the structure, their amplitude gradually decreases by almost three times compared to the structure without a DVD (**Figure 9**). In addition to reducing the amplitude of oscillations, the presence of a dynamic damper in the structure slightly increases the oscillation period of the "high-rise structure–dynamic damper" system, which is explained by the increase in the mass of the structure due to the installation of an additional mass of the DVD.

Next, for the calculation, damped kinematic effects were taken into account that can occur when loading the structure with seismic, explosive, and other long-term non-stationary impacts of the following type:

$$z = 0 : \ddot{u}_0 = A \sin(pt) \exp(-\gamma t). \tag{23}$$

Here, A is the amplitude of the impact; $p \approx \omega_0$ is the frequency of the impact equal to the first frequency of the bending natural oscillation modes of the structure; and $\gamma = 0.1$ is the coefficient characterizing the attenuation of the impact over time.

This is done to enable comparison of the displacements obtained in all cases and to analyze the influence not of the effect intensity, but of its nature on them:

$$A = \frac{\sqrt{p^2 + \gamma^2} \exp\left(\frac{\gamma}{p} \mathrm{arctg} \frac{p}{\gamma}\right)}{p} \tag{24}$$

Figure 10 shows the results obtained under damped harmonic impact (with a frequency close to the frequency of natural oscillations of the HRS-DVD system of a viscoelastic structure with a viscoelastic dynamic damper to assess the effect of oscillation damping. As seen from the results (**Figure 10**), as the intensity of the impact decreases, oscillations with a constant amplitude are observed for some time in the structure without a DVD, and in the HRS-DVD system, the oscillation amplitudes decrease sharply.

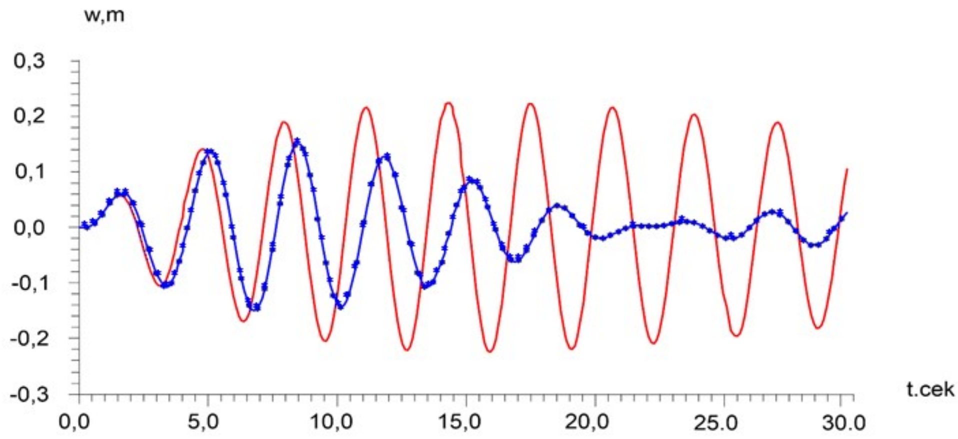

Figure 10. Change in the displacement of the upper point (z = 325 m) of the structure under a damped harmonic impact with a frequency close to the frequency of natural oscillations of the HRS-DVD system: structure without DVD (red curve); structure with DVD (blue curve with dots).

Figure 11 shows the dynamic behavior of a high-rise structure under real seismic action, i.e., the horizontal component of the accelerogram of the Gazli earthquake (1971) [32].

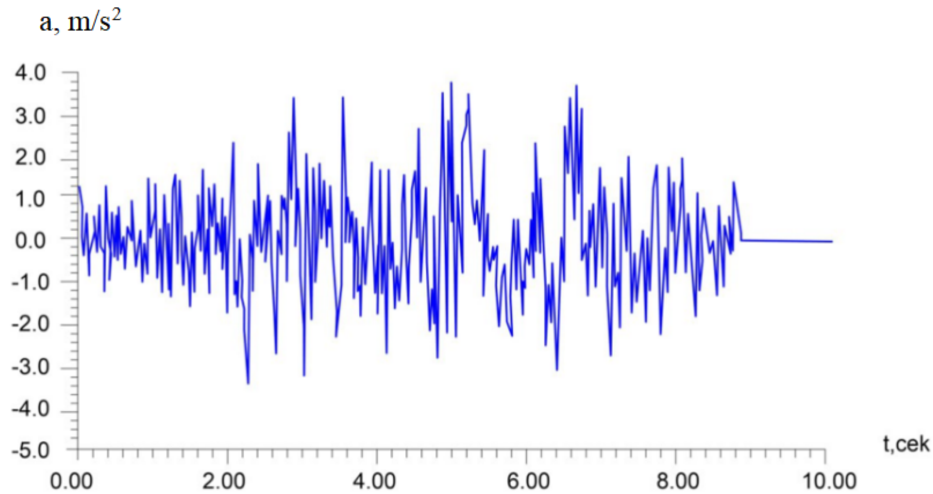

Figure 11. Horizontal component of the Gazli earthquake accelerogram.

The results show (**Figure 12**) that this high-frequency impact (as is known, the Gazli earthquake accelerogram belongs to this type of accelerogram since its predominant period is about 0.1 s) does not cause significant vibrations in a high-rise structure with a main vibration period of about 3 s. After the impact ceases (at t > 8.74 s), the structure is in the mode of free damped vibrations, and the effect of the damper in this case is insignificant.

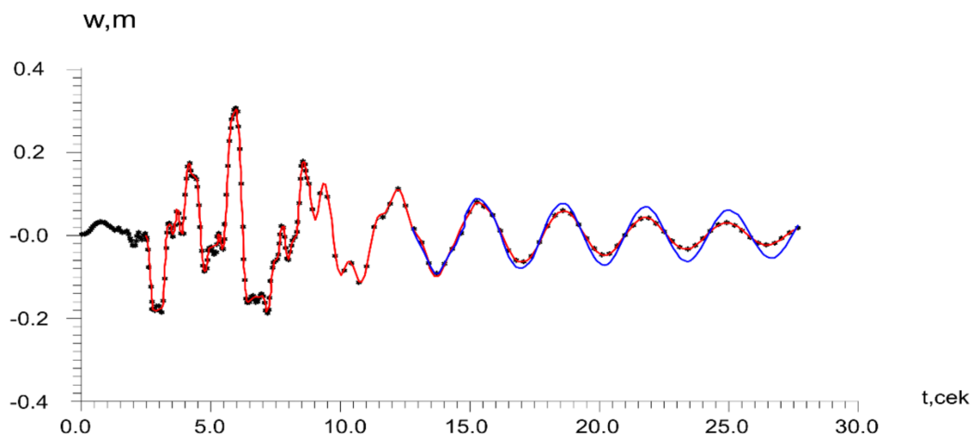

Figure 12. Change in the displacement of the upper point (z = 325 m) of a structure with a DVD considering the viscoelastic properties of the material and the damper spring under real seismic impact: stack without DVD (blue curve); stack with DVD (red curve with dots).

Thus, it is shown that for the effective operation of a dynamic damper, it is necessary first to tune it to the frequency of the structure and second to the frequency of the impact. Moreover, the longer the impact, the less effective the vibration damping becomes. As demonstrated by the calculations for high-frequency impact, where the damper has almost no effect on the dynamic behavior of the structure, the effective operation of the damper should involve selecting parameters not only in relation to the fundamental frequency of the protected structure but also concerning the higher frequencies of the structure, which can respond to the expected high-frequency dynamic impact.

Thus, the obtained results indicate that a correctly tuned dynamic vibration damper reduces the amplitude of the steady-state vibrations and unsteady forced vibrations. Accounting for the viscoelastic properties of the HRS-DVD system somewhat enhances the damping effect. The optimal solution for maximum damping of high-rise structures can be a group damper, which contains dynamic dampers of different frequency spectra.

4. Conclusion

(1) A mathematical model, methodology, and numerical algorithm have been developed to evaluate the dynamic behavior of high-rise axisymmetric HRS-DVD systems, considering the dissipative properties of both the structure and the damper materials.

(2) The dissipative behavior of both the structural material and the DVD was modeled using the Boltzmann–Volterra hereditary theory of viscoelasticity.

(3) The methodology, algorithm, and computer program were developed using the finite element method (FEM) and complex arithmetic.

(4) The natural, steady-state, and transient oscillations of high-rise axisymmetric structures with DVDs were investigated for various DVD parameters and external influences.

(5) During steady-state forced oscillations of the system, it was established that:

a. At the first resonance, the oscillation amplitudes at various points of the structure can be reduced by almost half if both the structure and the DVD are non-uniformly viscoelastic.
b. Increasing the mass of the DVD does not always lead to a reduction in the amplitude of the structure's oscillations. This can sometimes transform the system into a weakly coupled system, meaning the frequency of the damper's natural oscillations decreases, causing the structure and damper to oscillate independently.
c. In cases of strong system coupling, maximum damping of the structure's vibration amplitude can be achieved with properly adjusted DVD parameters in heterogeneous viscoelastic systems.

(6) A study on transient forced vibrations of high-rise axisymmetric structures with DVDs under high-frequency loads reveals that the DVD has insufficient impact on the vibration process, as resonance does not occur in this situation. Consequently, the DVD is ineffective and does not provide a positive effect under high-frequency loads.

(7) In the case of unsteady forced vibrations, maximum damping of vibrations can only be accomplished with optimally configured damper parameters, following an initial study of the natural and steady-state forced vibrations of the HRS-DVD system.

(8) This methodology, along with the computer calculation program, can be effectively utilized to evaluate the dynamic behavior of high-rise axisymmetric systems that include both a high-rise structure and a DVD. The results obtained from this evaluation can be applied to the design of high-rise structures with dynamic vibration dampers.

Author contributions: The authors contributed equally to this work. All authors have read and agreed to the published version of the manuscript.

Funding: This research received no external funding.

Institutional review board statement: Not applicable.

Informed consent statement: Not applicable.

Data availability statement: Data is contained within the article.

Acknowledgement: The research presented in this scientific article was conducted and developed within the framework of grant No. FZ-20200929327 "Development of a theory and method for assessing the strength and reliability of earth dams taking into account soil moisture and nonlinear filtration", carried out at the Department of Mechanics and Computer Modeling of the National Research University.

Conflict of interest: The authors declare no conflict of interest.

AI use statement: The authors declare that no artificial intelligence (AI) tools were used in the preparation of this manuscript.

References

1. Allena P, Bhavani Chowdary T. Effect of Irregularities on Seismic Performance of High Rise Structures. IOP Conference Series: Materials Science and Engineering. 2020; 998(1): 012064. doi: 10.1088/1757-899X/998/1/012064
2. Ivankova O, Stellmach M, Konecna L. Analysis of Asymmetric High-Rise Building. Key Engineering Materials. 2017; 738: 120–129. doi: 10.4028/www.scientific.net/KEM.738.120
3. Aihemaiti A, Todorovska MI, Trifunac MD, et al. The effects of the environmental conditions on the modal frequencies, damping ratios and curvatures of a 50-story skyscraper. Soil Dynamics and Earthquake Engineering. 2026; 200: 109801. doi: 10.1016/j.soildyn.2025.109801
4. Foroutan K, Dai L. Chaos and resonance of nonlinear FG shallow shells reinforced by oblique stiffeners. Thin-Walled Structures. 2024; 205: 112402. doi: 10.1016/j.tws.2024.112402
5. Xue Y, Hao W. Extracting nonlinear aerodynamic damping of crosswind-excited tall buildings based on probability density function of displacement amplitude. Journal of Building Engineering. 2023; 72: 106632. doi: 10.1016/j.jobe.2023.106632
6. Patil RA, Salgar PB. An investigation for enhancing seismic performance of high-rise buildings using fluid viscous damper (FVD). Asian Journal of Civil Engineering. 2024; 25(6): 4803–4817. doi: 10.1007/s42107-024-01081-1
7. Tudu C, Patnaik M, Bagal DK. Assessing the efficacy of tuned mass dampers in mitigating wind-induced vibrations of tall structures. Innovative Infrastructure Solutions. 2024; 9(6): 193. doi: 10.1007/s41062-024-01511-8
8. Mondrus VL, Paramonov EE, Panov MA. Linear and nonlinear oscillation dampers in the vibration protection system of buildings. Building and Reconstruction. 2026; (2): 19–33. doi: 10.33979/2073-7416-2026-124-2-19-33 (in Russian)
9. Legeza VP. Dynamic Analysis of the Behavior of a Pendulum Damper with Mobile Suspension Point. International Applied Mechanics. 2022; 58(3): 327–335. doi: 10.1007/s10778-022-01158-x
10. Legeza VP, Neshchadym OM. Mathematical model of the damped process of longitudinal impacts in a system with dry friction shock absorbers. Scientific notes of Taurida National V.I. Vernadsky University. Series: Technical Sciences. 2024; 1(1): 195–202. doi: 10.32782/2663-5941/2024.1.1/30 (in Russian)
11. Legeza VP. Efficiency of the Pendulum Damper with a Mobile Suspension Point. Strength of Materials. 2022; 54(2): 222–232. doi: 10.1007/s11223-022-00395-2
12. Aly AM, Chapain S. Seismic response reduction using a tuned pendulum pounding mass damper: Experimental verification of superior performance. Soil Dynamics and Earthquake Engineering. 2023; 173: 108044. doi: 10.1016/j.soildyn.2023.108044
13. Akyürek O. Analysis of Different Placement Strategies of Multi-Tuned Mass Dampers Placed in Building Height. Arabian Journal for Science and Engineering. 2023; 48(4): 5447–5465. doi: 10.1007/s13369-022-07440-x
14. Kontoni DPN, Farghaly AA. Seismic control of vertically and horizontally irregular steel high-rise buildings by tuned mass dampers including SSI. Asian Journal of Civil Engineering. 2024; 25(2): 1995–2014. doi: 10.1007/s42107-023-00890-0
15. Quintana Gallo P, Carradine DM, Bazaez R. State of the art and practice of seismic-resistant hybrid timber structures. European Journal of Wood and Wood Products. 2021; 79(1): 5–28. doi: 10.1007/s00107-020-01556-3
16. Ding H, Wang JT, Lu LQ, et al. Experimental comparison of nonlinear damping performance of toroidal and conventional tuned liquid column dampers. Nonlinear Dynamics. 2021; 104(4): 3365–3384. doi: 10.1007/s11071-021-06552-7
17. Brownjohn JMW. Long-term monitoring of dynamic response of a tall building for performance evaluation and loading characterization. In: Proceedings of the 1st International Operational Modal Analysis Conference; 26–27 April 2005; Copenhagen, Denmark. pp. 143–154.
18. Brownjohn JMW, Au S, Wang X, et al. Bayesian operational modal analysis of offshore rock lighthouses for SHM. In: Proceedings of the 9th European Workshop on Structural Health Monitoring; 10–13 July 2018; Manchester, UK.
19. Brownjohn JMW, Carden EP, Goddard CR, et al. Real-time performance monitoring of tuned mass damper system for a 183m reinforced concrete chimney. Journal of Wind Engineering and Industrial Aerodynamics. 2010; 98(3): 169–179. doi: 10.1016/j.jweia.2009.10.013
20. Górski P. Investigation of dynamic characteristics of tall industrial chimney based on GPS measurements using Random Decrement Method. Engineering Structures. 2015; 83: 30–49. doi: 10.1016/j.engstruct.2014.11.006

21. Xiong C, Niu Y. Investigation of the Dynamic Behavior of a Super High-rise Structure using RTK-GNSS Technique. KSCE Journal of Civil Engineering. 2019; 23(2): 654–665. doi: 10.1007/s12205-018-0238-9
22. Elias S, Matsagar V, Datta TK. Distributed Tuned Mass Dampers for Multi-Mode Control of Benchmark Building under Seismic Excitations. Journal of Earthquake Engineering. 2019; 23(7): 1137–1172. doi: 10.1080/13632469.2017.1351407
23. Safarov II, Teshayev MH, Juraev SI, et al. Vibrations of Viscoelastic Plates with Attached Concentrated Masses. Lobachevskii Journal of Mathematics. 2024; 45(4): 1729–1737. doi: 10.1134/S1995080224601474
24. Alhasan AA, Vafaei M, C Alih S. Viscoelastic dampers for protection of structures against seismic actions. Innovative Infrastructure Solutions. 2022; 7(5): 309. doi: 10.1007/s41062-022-00905-w
25. Liao X, Chen L, Lee H, et al. Dynamic performance of a novel hydraulically damped rubber mount with inertial track at low frequency: modeling and experimental study. Journal of Mechanical Science and Technology. 2023; 37(12): 6325–6342. doi: 10.1007/s12206-023-1109-y
26. Wang X, Zhu Z, Au SK. Bayesian operational modal analysis of structures with tuned mass damper. Mechanical Systems and Signal Processing. 2023; 182: 109511. doi: 10.1016/j.ymssp.2022.109511
27. Arabzai S, Ahmad M, Sajid M, et al. Advanced damping devices for tall buildings under seismic and wind loads: A state-of-the-art review. Architecture, Structures and Construction. 2026; 6(1): 9. doi: 10.1007/s44150-026-00192-4
28. Kim DH, Ju YK, Kim MH, et al. Wind-induced vibration control of tall buildings using hybrid buckling-restrained braces. The Structural Design of Tall and Special Buildings. 2014; 23(7): 549–562. doi: 10.1002/tal.1066
29. Zhong C, Chen Y, Sang L, et al. Advances in Wind-Induced Vibration Control of High-Rise Buildings. In: Ma J, Masrour R, Gloria A, et al. (editors). Advances in Machinery, Materials Science and Engineering Application XI. IOS Press; 2025. pp. 661–667. doi: 10.3233/ATDE251045
30. Zhao L, Yang Q, Guo K, et al. Investigation on three-dimensional coupled vibration in wind-structure interaction of high-rise structures using fully-coupled numerical simulation. Engineering Structures. 2026; 357: 122595. doi: 10.1016/j.engstruct.2026.122595
31. El Ouni MH, Abdeddaim M, Elias S, et al. Review of Vibration Control Strategies of High-Rise Buildings. Sensors. 2022; 22(21): 8581. doi: 10.3390/s22218581
32. Kang X, Tang J, Wei J, et al. Parameter optimization of vibration control system for adjacent building structures based on negative stiffness inerter damper. Scientific Reports. 2024; 14(1): 8742. doi: 10.1038/s41598-024-59380-1
33. Mirsaidov M, Khudainazarov S. Spatial natural vibrations of viscoelastic axisymmetric structures. Magazine of Civil Engineering. 2020; 96(4): 118–128.
34. Khudainazarov S, Donayev B, Sabirjanov T, et al. Non-stationary vibrations of a viscoelastic structure. AIP Conference Proceedings. 2023; 2612: 020015. doi: 10.1063/5.0113281
35. Mirsaidov M, Abdikarimov R, Khudainazarov S, et al. Damping of high-rise structure vibrations with viscoelastic dynamic dampers. E3S Web of Conferences. 2020; 224: 02020. doi: 10.1051/e3sconf/202022402020
36. Filatov AN. Asymptotic Methods in the Theory of Differential and Integro-Differential Equations. FAN; 1974. (in Russian)
37. Koltunov MA. Creep and Relaxation. Vysshaya Shkola; 1976. (in Russian)
38. Atkinson KE. An Introduction to Numerical Analysis, 2nd ed. John Wiley & Sons; 1989.
39. Lukashevich AA. Modern Numerical Methods of Structural Mechanics: A Textbook. Publishing House of Khabarovsk State Technical University; 2003. (in Russian)
40. Newmark NM. Inelastic Design of Nuclear Reactor Structures and Its Implications on Design of Critical Equipment. IASMiRT; 1977.